Design and Implementation of a Robotic Shark with a Novel Embedded Vision System

Xiang Yang, Zhengxing Wu and Junzhi Yu

Abstract— **This paper focuses on the mechatronic design and control issues of a novel robotic shark with an embedded vision system. To pursue a better swimming performance, an updated robotic shark with more degrees of freedom (DOFs) is constructed. Specially, an optimized propulsive mechanism with three links is designed to fit a typical shark-like swimming and a pair of pectoral fins with two separate DOFs is employed to regulate both pitch attitude and roll attitude. In order to strengthen the capability of underwater perception, an embedded vision system is fixed in the robotic shark. Besides, a particular camera stabilizer with an Inertial Measurement Unit (IMU) is designed to counteract the head swing for high-quality images. Moreover, a CPGs-govern control strategy is adopted to realize various shark-like locomotion and further analysis are executed to explore the relationship between propulsive performance and some key characteristics of adopted CPGs. Finally, the robotic shark successfully realizes more flexible shark-like locomotion containing forward swimming, turning, diving and surfacing. The experimental results validate the effectiveness of the updated mechatronic design and adaptability of sharklike swimming governed by CPGs.**

I. Introduction

The bio-inspired mechatronic system has gathered much attention in both academia and industry over the last two decades [1]. As a typical bio-inspired mechatronic system, robotic fish has been extensively researched since the first prototype, RoboTuna, was developed at MIT in 1995 [2]–[4]. Biologists always employ the robotic fish as an excellent auxiliary platform to study the kinematic mechanism and hydrodynamic analysis of fishlike swimming [5]. Meanwhile, engineers develop the robotic fish as a special underwater vehicles to explore a practical and flexible propulsive mechanism, since the robotic fish has shown superior propulsive performance including high maneuverability and low noisy, compared with traditional man-made propellers [6]–[8]. According to specially designed features, a robotic fish can execute a range of tasks, such as underwater exploration, search and recovery, as well as military missions.

In nature, most fish generate propulsive thrust depending on their flexible body and caudal fin, termed body and/or caudal fin (BCF) propulsion, and other fish utilize their median and pectoral fins to realize swimming, termed median and/or pared fin (MPF) propulsion [9]. No matter which mode the fish employ for propulsion, most fish all need a kind of similar rhythmic signals, which are always governed by a neural network, Central Pattern Generators (CPGs). Biologically, CPGs are neural networks usually located in the spinal cord of vertebrate animals [10] which are responsible for generating cyclic muscle activation patterns such as respiration, chewing, walking and crawling [11], [12]. Inspired by this biological phenomenon, more and more researchers employ CPGs to generate fishlike swimming pattern recently [13]. Compared with the traditional fish-body-wave method, CPGs as online gait generators, have many advantageous including strong robustness, smooth transition process, good adaptability and easily adjustable output [14]. When some key parameters are suddenly changed, the CPGs have excellent qualities to keep smooth and continuous. Moreover, the CPGs are easily applied for the robotic fish because of their mechanical structures. Therefore, the CPGs method is a perfect choice to realize fishlike swimming, such as forward swimming, turning, diving and surfacing.

Generally, almost all daylight fish have color vision just as well as human eyes. Though underwater vision is not a primary sense for fish, it still plays an important role in predator-prey interaction. As for robotic fish, the underwater vision system is a very important instrument for better understanding of environment. Thus, the robotic fish with an embedded vision system can become more intelligent and easily accomplish more complicated missions, such as target tracking, localization, formation control, and cave searching [15]–[17]. In previous works, many researches have focused on the robotic fish vision system. However, an important problem about the instability caused by the sway of the robotic fish while swimming is still unsolved. Considering the pan/tile camera is widely applied in the vision system of Unmanned Aircraft System (UAS) [18], we design a similar mechanism for the embedded vision system of a small robotic fish to improve the image quality.

In our previous work [19], a small robotic shark with multiple sensors including a gyroscope, a pressure sensor, three infrared sensors and a light sensor was developed. Based on bio-inspired CPG-centred control methods, the robotic shark successfully realized three-dimensional motions and light navigation. On the basis of previous research, an updated robotic shark which has more flexible propulsive mechanism and more effective sensors is proposed in this paper. Different with previous version, the updated robotic shark employs a three-link hinge propulsive mechanism for more flexible shark-like swimming, especially turning maneuvers. Besides, an updated pectoral fins with two degrees of freedom (DOFs)

*This work was partly supported by the National Natural Science Foundation of China (61375102, 61333016, 61573226,61603388,61633017), the Beijing Natural Science Foundation (3141002, 4164103, 4161002) and the Early Career Development Award of SKLMCCS.

Xiang Yang, Zhengxing Wu and Junzhi Yu are with the State Key Laboratory of Management and Control for Complex Systems, Institute of Automation, Chinese Academy of Sciences, Beijing 100190, China.

(e-mail: zhengxing.wu@ia.ac.cn)

is developed to regulate not only pitch attitude but also roll attitude. More importantly, the robotic shark employs a novel embedded camera system with a camera stabilizer to enhance the capability of perception in underwater environment. Finally, the robotic shark successfully realizes more flexible motions including forward swimming, backward swimming, turning, diving and surfacing. The experimental results validate the effectiveness of the mechatronic design of the updated robotic shark.

In the rest of this paper, the overall mechatronic description of the updated robotic shark is overviewed in Section II. Section III introduces the adopted CPG model and control strategies. Some revelent experiments are further provided in Section IV. Finally, Section V concludes the paper with an outline of future work.

II. Mechatronic Design of the Robotic Shark

With the purpose of high maneuverability, an updated robotic shark prototype with several new mechanical features is designed. Fig. 1 presents the developed robotic shark prototype. The robotic shark consists of a rigid anterior body with one pair of pectoral fins, and a multi-articulated posterior body with a lunate caudal fin. In order to be installed conveniently, the head shell, made of acrylonitrile–butadiene–styrene copolymer (ABS), is divided into upper and lower portions. And the head has a relative big space to housing control circuits, batteries, sensors, a camera with camera stabilizer and pectoral mechanism. Different from the previous version, the updated robotic shark employs a pair of pectoral fins with two separate DOFs. Thus, the robotic shark can easily control both pitch attitude and roll attitude for better maneuverability. The propulsive posterior body adopts three powerful servomotors for a better fitting curves of a shark swimming. Generally, the robotic shark has 483 mm long, and weights about 1.3 kg. Table. I gives a detailed technical specification of the robotic shark.

A. Anterior Body Design

Shark, as a kind of fierce predator living in the sea, has a well-streamlined body shape, which provides the magnificent swimming performance. For the purpose of reproducing the excellent swimming performance of sharks, a robotic fish mimicking sharks is developed. In order to protect the circuits and batteries inside the robotic shark from the water, a proper waterproof design is required. Moreover, the anterior body shell is divided into upper and lower parts for installation convience. As shown in Fig. 2, the upper one is convex for getting a bigger cross section. An O-ring made of fluoride rubbers is employed for sealing. By removing the upper shell, all components inside the robotic shark can be easily replaced or repaired.

In order to strengthen the underwater perception, an embedded vision system is built in the anterior body shell. For a robotic shark in swimming, the head always sways inevitably because of the counterforce on the posterior body and caudal fin, which results in severe blur of image. Moreover, the camera might lose target object during the swaying because

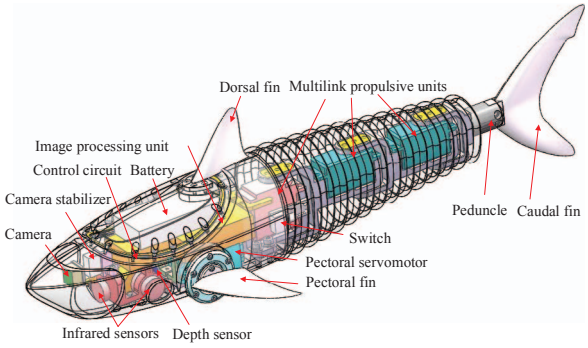

(a) Conceptual design

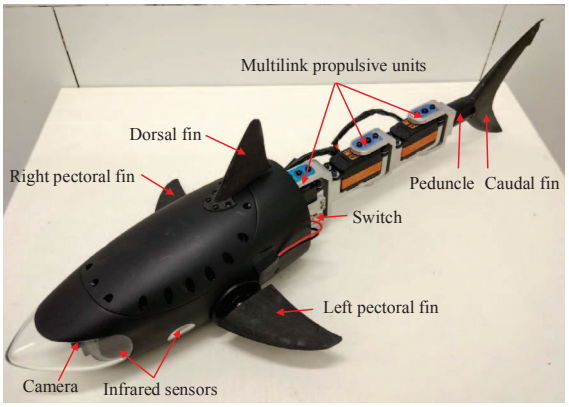

(b) Robotic shark prototype

Fig. 1. Mechanical design of the updated robotic shark.

TABLE I
Technical Specification of the Developed Robotic Shark.

Items	Characteristic
Size($L \times W \times H$)	$\sim 483 \times 208 \times 125\ mm^3$
Total mass	~ 1.3 kg
Drive mode	Servomotors (HS-7940TH, SAVOX-1251TG)
Sensors	Infrared sensor, Pressure sensor, IMU, Camera
Controller	ARM Cortex-M4
Operating voltage	DC 7.4V

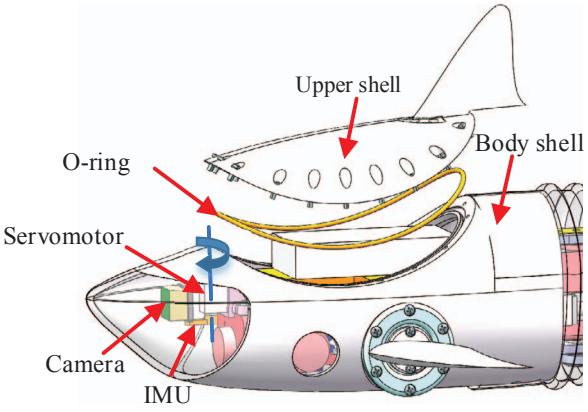

Fig. 2. Mechanical design of the anterior body shell.

of the small field of vision. For the purpose of reducing the blur of image and getting a larger field of vision, a novel mechanism for stabilizing the camera, i.e. camera stabilizer,

is proposed. As shown in Fig. 2, the camera stabilizer has a motor rotating around the yaw axis, which is responsible for controlling the yaw angle of the camera mounted on the camera. Generally speaking, a pan/tilt camera has at least two DOFs, which is the ideal profile for camera stabilizer. However, the limited size inside the robotic shark makes the design of a two-DOFs camera stabilizer very difficult, thus a one-DOF camera stabilizer is adopted. An IMU is mounted on the camera stabilizer along with the camera to get the yaw angle of the camera, which provides feedback for the controller of camera stabilizer.

B. Pectoral Fins

Pectoral fins of fish have extremely complex structure which provides fish with fast and maneuverable locomotion ability. Many complex pectoral mechanisms with multi-DOFs were developed to study the drive principle and hydrodynamic behaviors [20]. Nevertheless, it is almost impossible to employ such kind of complex mechanisms inside a small size robotic shark because of the limited space. Simple mechanisms of pectoral fins are employed in this paper. Each pectoral fin is driven by one servomotor, which yields two DOFs for two pectoral fins. By changing the pitch angle of pectoral fins, motions such as diving, ascending and rolling can be accomplished. The waterproof design is another concern for pectoral fins. Since there is a rotating shaft in each pectoral fin, it is an optimal choice to use the Glyd ring for dynamic sealing. Besides, assembling posts another problem for mechanism design since it is very hard to assemble two pectoral fins with long shafts and the body shell. For the convenience of assembling, a dynamic sealing lid with a bearing and a Glyd ring is designed for each pectoral fin, which is shown in Fig. 3. With the dynamic sealing lid, the two servomotors of pectoral fins can be put inside the body shell first, and then assemble the lids and the body shell.

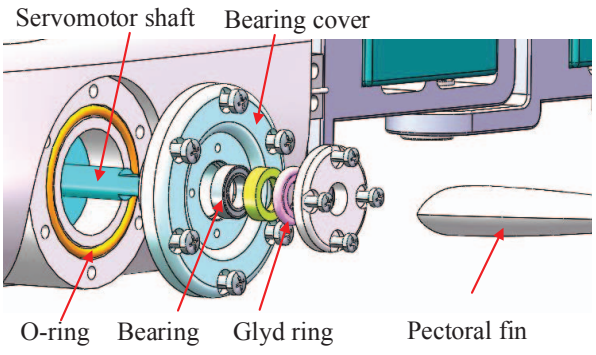

Fig. 3. Waterproof Design of the pectoral fins.

C. Multilink Propulsive Mechanism

The propulsive module of robotic shark still employs multilink hinge structure like before. Different with the previous version, the updated robotic shark adopts more joints to produce sharklike swimming gaits and also to pursue high maneuverability especially turning maneuvers. Specifically, three flexible links actuated by servomotors are connected in series with aluminum skeletons. To mimicking the shape of a real shark, two servomotors with smaller size is adopted for the two hinges close to the caudal fin. Besides, as an update version, better servomotors with stronger torque and higher turning speed is adopted to pursue a better performance.

III. Locomotion Control

A. CPG Model

Considering a robotic shark propels itself through a rhythmic right-to-left movement of the posterior body with a caudal fin, a CPG-based model is very suitable for its locomotion control. The applied CPGs model is shown as follows [21],

$$\begin{cases} \dot{\theta}_i = 2\pi\upsilon_i + \sum\limits_{j\in T(i)} \omega_{ij}\sin\left(\theta_j - \theta_i - \phi_{ij}\right) \\ \ddot{r}_i = a_i\left(\dfrac{a_i}{4}\left(R_i - r_i\right) - \dot{r}_i\right) \\ x_i = r_i\left(1 + \cos\theta_i\right) \end{cases} \tag{1}$$

where θ_i and r_i represents the phase and amplitude of the ith oscillator, υ_i and R_i are the intrinsic frequency and amplitude, a_i is a positive constant and ω_{ij} and ϕ_{ij} determine the weights and phase biases of coupling between the ith and jth oscillators. $T\left(i\right)$ is the set of oscillators that the ith oscillators receives inbound couplings from. x_i is the rhythmic output of the ith oscillator. The output angle φ_i of the ith servomotor can be obtained by the following equation:

$$\varphi_i = x_i - x_{3+i} \tag{2}$$

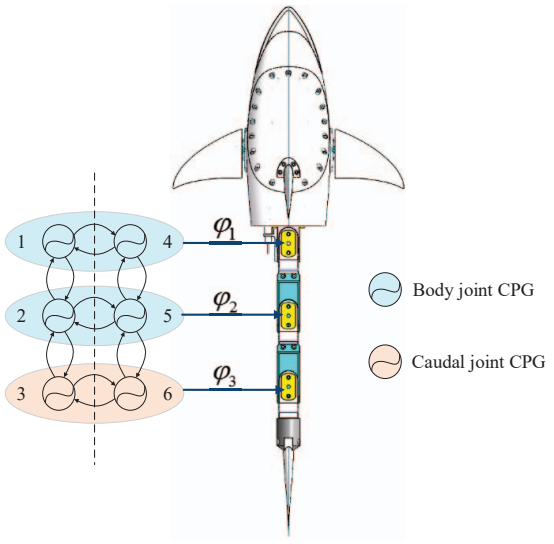

Fig. 4. The topography of the CPG network applied in the robotic shark.

Specifically, the CPG model in this paper consists of two chain of oscillators that couple with nearest neighbor, which is shown in Fig. 4. There are 6 oscillators in the CPG model in total. Every joint of the multilink hinge is provided with two oscillators to produce sinusoidal signal to drive the

servomotor. The joints from head to tail are numbered 1 to 3. Oscillators in the left are numbered 1 to 3, and these in the right are numbered 4 to 6 from head to tail.

For the sake of simplicity, several parameters of CPGs are set to the same value, such as $\upsilon_i = \upsilon$, $\omega_{ij} = \omega$ and $a_i = a$ for all oscillators. The phase biases between the left and right oscillators of joints are set to π, which means they oscillate in antiphase. The phase biases between oscillators belonging to different joints are set to $\Delta\phi$ for the descending connections and $-\Delta\phi$ for ascending connections. The parameter $\Delta\phi$ represents the phase lag between neighbor joints. Though phase lags between all neighbor joints are set to the same value, it is proper for our robotic fish since the distance between neighbor joints are the same. With all these settings, the CPG model yields signal for the set point of angles of servomotors of every joints, which asymptotically converge to (3).

$$\begin{aligned}\varphi_i{}^{\infty}(t) = &(A_{Li} - A_{Ri}) \\ &+ (A_{Li} + A_{R_i}) \cos(2\pi\upsilon t + i\Delta\phi + \phi_0)\end{aligned} \tag{3}$$

where A_{Li} and A_{Ri} are the intrinsic amplitudes of the left and right oscillators, ϕ_0 depends on the initial state of the oscillators. As can be seen from (3), $(A_{Li} - A_{Ri})$ represents the offset and $(A_{Li} + A_{Ri})$ represents the amplitude of the ith joint. Assuming that we want to set the offset and amplitude as δ_i and A_i, we should set $A_{Li} = (A_i + \delta_i)/2$ and $A_{Ri} = (A_i - \delta_i)/2$.

In brief, we could set the frequency, phase lag, amplitude and offset of the sinusoidal signal for controlling the angle of servomotor by altering υ, $\Delta\phi$, A_i and δ_i. In this paper, we set $\omega = 4, a = 100, A_1 = 20\pi/180, A_2 = 29\pi/180, A_3 = 38\pi/180$.

Other parameters are set to different values depending on different motions. An example of how the CPG responses to sudden change of parameters are shown in Fig. 5. The output of the oscillators smoothly converge to the new waveform without any discontinuities.

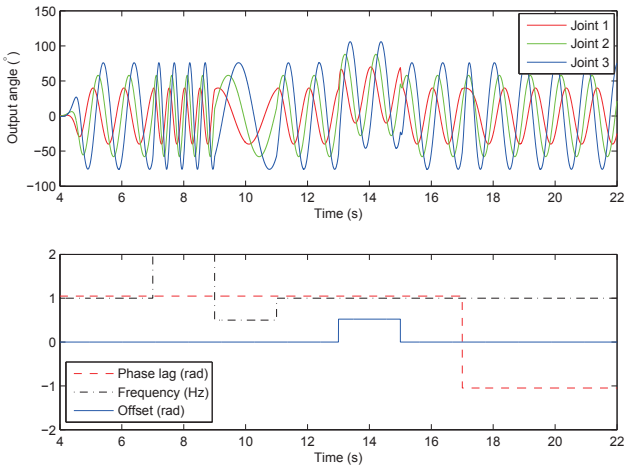

Fig. 5. The CPGs output signals responding to some sudden change of parameters.

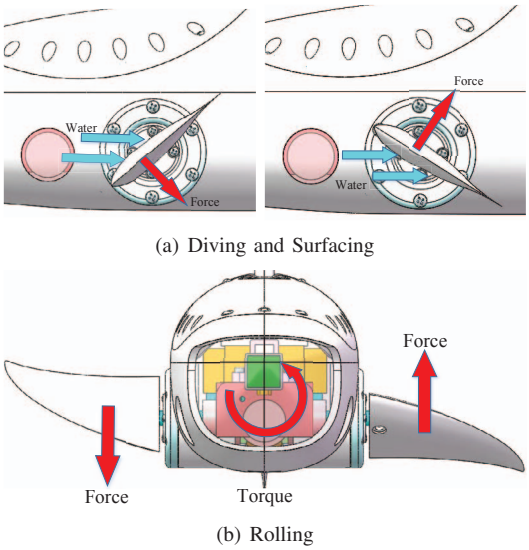

(a) Diving and Surfacing

(b) Rolling

Fig. 6. Schematic of performing motions with pectoral fins.

B. 3D Motion Control

With the CPG model, the robotic shark is capable to swim forward with the thrust from water generated by the rhythmic undulation of body parts. However, to control the 3D motion of a robotic shark including turning, diving, surfacing, rolling and backward swimming, the parameters of CPG model need to be altered and pectoral fins need to be used.

Generally speaking, the speed of robotic fish is changed by altering the frequency of body wave, i.e., the intrinsic frequency υ. When it comes to the turning motion, the offset δ_i is used. For simplicity, we set $\delta_i = \beta A_i$, where β is the offset ratio for all joints. If the robotic shark needs to turn left, a positive β should be adopted. If the robotic shark needs to turn right, a negative β should be taken. When the robotic shark is commanded to swim straight, β should be set to 0. The diving, surfacing and rolling motions demand a certain speed of robotic fish and the aid of pectoral fins. In particular, when the robotic shark swims at a certain speed with its pectoral fins heading down (as shown in the left figure of Fig. 6(a)), the water will generate a downward force on the pectoral fins, which will make the robotic shark swim downward. For surfacing motion, the angle of pectoral fins should be set as the right figure of Fig. 6(a), which will generate a upward force for robotic fish to swim upward. With one pectoral fin heading downward and the other one heading upward (as shown in Fig. 6(b)), the force on pectoral fin yields torque that drives robotic shark to roll along the head-tail axis, which enables robotic shark to carry out rolling motion. As for backward swimming motion, simply reversing the phase lag of the CPG model can generate backward thrust for swimming [22]. With the capability of forward swimming, backward swimming, turning, diving, surfacing and rolling, robotic fish is able to reach any position with any attitude.

IV. Experiments and Results

For the purpose of evaluating the mechatronic design and control method of the developed robotic shark, extensive experiments are carried out. Note that since detail design and evaluation of the camera stabilizer has been given in our previous work [23], this paper mainly focuses on the swimming performance of the robotic shark.

A. Experimental Setup

In order to precisely measure the planar motion of the robotic shark, a motion measurement system based on a global vision system is introduced [24]. Generally, the whole experiments are carried out in a lab pool with 500 cm long, 400 cm wide, and 120 cm deep. The camera of the motion measurement system locates about 190 cm above the water and timely records the robotic shark swimming, Then, a self-developed motion measurement software in the host PC detects its swimming position according to the video information from the camera. Moreover, a radio frequency (RF) module is adopted to communicate with the robotic shark. Fig. 7 illustrated the whole schematic.

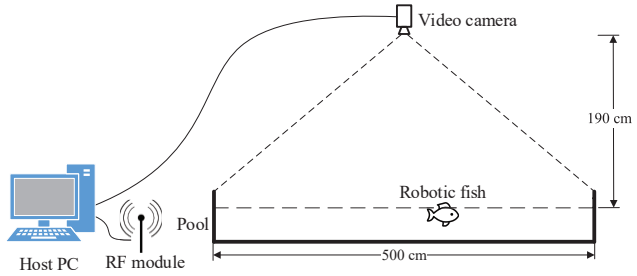

Fig. 7. Schematic of the motion measurement system.

The first experiment concerned on the forward swimming speed evaluation. The parameters of CPG model were set as $\omega = 4, a = 100, A_1 = 20\pi/180, A_2 = 29\pi/180, A_3 = 38\pi/180$. Then, through changing some key characteristics of the CPGs, we explored how the applied CPGs affected the swimming performance of the robotic shark. Specially, the swimming speeds were respectively measured in the conditions of six different frequencies ($\upsilon = 0.5, 0.75, 1.0, 1.25, 1.5, 1.75$ Hz) and five different phase lags($\Delta\phi = 30°, 45°, 60°, 75°, 90°$). Fig. 8 plots the forward swimming speed with varying frequencies and phase lags. It is clear that the final propulsive speed increases with an increasing frequency but with a decreasing phase lags over $60°$. When the phase lags is smaller than $60°$, the swimming speed has no obvious different, see the speed curves when $\Delta\phi = 30°, 45°, 60°$ in Fig 8. Besides, we also found that small phase lags would cause an acute head swaying with a large amplitude of the robotic shark, which was disadvantageous for the vision system inside the robotic shark. Therefore, we think a larger phase lag is a better choice for the robotic shark, e.g. $\Delta\phi = 60°$.

The second experiment focused on the turning maneuvers. Through changing the offset ratios ($\beta = 0.2, 0.4, 0.6, 0.8$) in

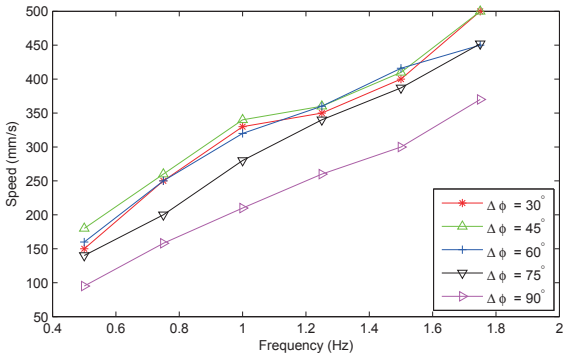

Fig. 8. Speeds with varying frequencies and phase lags.

CPGs, we can obtain that the robotic shark gets a bigger turning speed and a smaller turning radius when a larger offset ratio is given. Finally, the robotic fish achieved a turning speed to 3.8 rad/s following a turning radius of 198 mm at $\beta = 0.8$ and frequency of 1 Hz, as shown in Fig. 9. Fig. 10 shows the turning trajectory of the robotic shark drawn by the applied motion measurement system. Moreover, a diving and surfacing experiment was also executed to test the three-dimensional locomotion capability of the robotic shark, as shown in Fig. 11. According to these extensive experiments, we can see that the robotic shark can successfully realize various locomotion including forward swimming, turning, diving and surfacing.

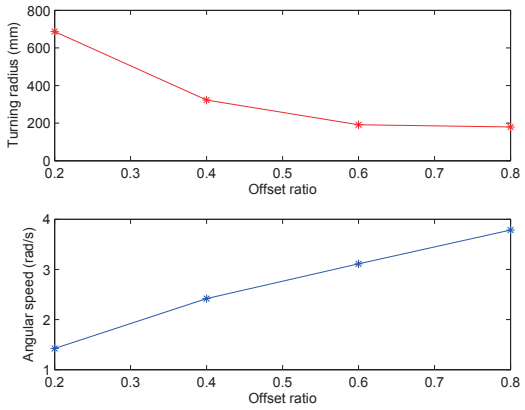

Fig. 9. Angular speeds and turning radiuses with varying offset ratios.

V. Conclusions and Future Work

In this paper, we have developed an updated robotic shark with multiple sensors. In order to enhance the swimming performance, the updated robotic shark employs more powerful and flexible propulsive mechanism. Specially, an optimized three-link hinge structure is designed to fit the shark swimming body curves and a pair of flexible pectoral fins with two DOFs is adopted to provide more powerful capability of three-dimensional swimming, *e.g.* regulating the pitch attitude and roll attitude when swimming. Moreover,

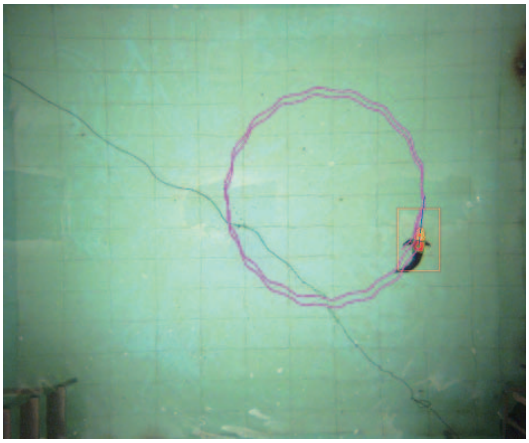

Fig. 10. Snapshot sequence of the turning.

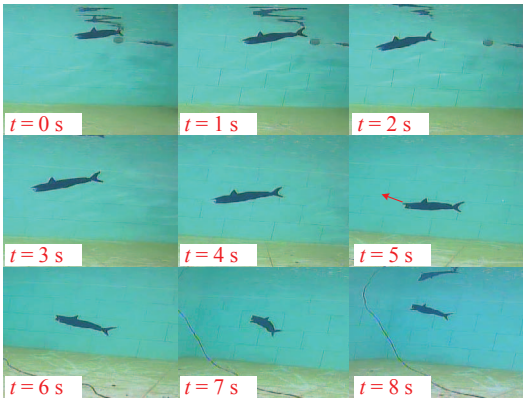

Fig. 11. Snapshot sequence of the diving and surfacing motion.

an embedded vision system with a camera stabilizer is developed to eliminate the image degeneration caused by the swaying of the robotic shark head. As for the control level, a CPGs-based control strategy is employed to realize various locomotion such as forward swimming, turning, diving and surfacing. Meanwhile, further discussion about how the key parameters of the applied CPGs model including frequency, phase lag and offset affect the swimming performance is held. Finally, the developed robotic shark realized better swimming performance such as flexible and fast turning. The experimental results validate the effectiveness of the improved mechatronic design and CPGs-governed control strategy for sharklike swimming.

The ongoing and future work will focus on target tracking of the robotic shark with an embedded vision system in field underwater environment. Specifically, with the help of the embedded vision system with a camera stabilizer, the robotic shark can obtain clear images containing abundant information of the underwater environment. Along with other sensors, the robotic shark could carry out some special tasks, including target searching, trajectory tracking, obstacle avoiding and so on.

REFERENCES

[1] N. F. Lepora, P. Verschure, and T. J. Prescott, "The state of the art in biomimetics," *Bioinspiration & Biomimetics*, vol. 8, no. 1, Article ID 013001, 11 pages, 2013.

[2] M. S. Triantafyllou, and G. S. Triantafyllou, "An efficient swimming machine," *Scientific American,* vol. 272, no. 3, pp. 40–48, 1995.

[3] F. E. Fish, Advantages of natural propulsive systems, Marine Technology Society Journal, vol. 47, no. 5, pp. 37–44, 2013.

[4] J. Yu, M. Tan, S. Wang, *et al*, "Development of a biomimetic robotic fish and its control algorithm," *IEEE Transactions on Systems, Man, and Cybernetics, Part B (Cybernetics)*, vol. 34, no. 4, pp. 1798–1910, 2004.

[5] C. J. Esposito, J. L. Tangorra, B. E. Flammang, *et al*, "A robotic fish caudal fin: effects of stiffness and motor program on locomotor performance," *The Journal of Experimental Biology*, vol. 215, no. 1, pp. 56–67, 2012.

[6] C. Zhou, H. K. Low, "Design and locomotion control of a biomimetic underwater vehicle with fin propulsion," *IEEE/ASME Transactions on Mechatronics*, vol. 17, no. 1, pp. 25–35, 2012.

[7] T. Hu, H. K. Low, L. Shen, *et al*, "Effective phase tracking for bioinspired undulations of robotic fish models: a learning control approach," *IEEE/ASME Transactions on Mechatronics,* vol. 19, no. 1, pp. 191–200, 2014.

[8] J. He, Y. Zhang, and K. Low, "Comparative study of effect of fin arrangement on propulsion performance of bio-inspired underwater vehicles with multiple SMA fins," *International Journal of Advanced Robotic Systems,* doi: 10.5772/61392, 2015.

[9] M. Sfakiotakis, D. M. Lane, and J. B. C. Davies, "Review of fish swimming modes for aquatic locomotion," *IEEE Journal of oceanic engineering*, vol. 24, no. 2, pp. 237–252, 1999.

[10] P. A. Guertin, The mammalian central pattern generator for locomotion, *Brain Research Reviews*, vol. 62, no. 1, 2009.

[11] D. A. McCrea, and I. A. Rybak, "Organization of mammalian locomotor rhythm and pattern generation," *Brain research reviews*, vol. 57, no. 1, pp. 134–146, 2008.

[12] J. E. Rubin, N. A. Shevtsova, G. B. Ermentrout, *et al*, "Multiple rhythmic states in a model of the respiratory central pattern generator," *Journal of Neurophysiology*, vol. 101, no. 4, pp. 2146–2165, 2009.

[13] G. Wang, D. B. Zhang, L. X. Lin, *et al*, "CPGs control method using a new oscillator in robotic fish," *Science China Technological Sciences*, vol. 53, no. 11, pp. 2914–2919, 2010.

[14] A. J. Ijspeert, "Central pattern generators for locomotion control in animals and robots: a review," *Neural Networks*, vol. 21, no. 4, pp. 642–653, 2008.

[15] J. Yu, F. Sun, D. Xu, *et al*, "Embedded vision-guided 3-D tracking control for robotic fish," *IEEE Transactions on Industrial Electronics*, vol. 63, no. 1, pp. 355–363, 2016.

[16] W. Wang, and G. Xie, "Online high-precision probabilistic localization of robotic fish using visual and inertial cues," *IEEE Transactions on Industrial Electronics*, vol. 62, no. 2, pp. 1113–1124, 2015.

[17] S. F. Chen, and J. Yu, "Underwater cave search and entry using a robotic fish with embedded vision," in *Proc. 33rd Chinese Control Conference*, Nanjing, China, Jul. 2014, pp. 8335–8340.

[18] D. D. Doyle, A. L. Jennings, and J. T. Black, "Optical flow background estimation for real-time pan/tilt camera object tracking," *Measurement*, vol. 48, pp. 195–207, 2014.

[19] J. Yu, S. Chen, Z. Wu, *et al*, "On a miniature free-swimming robotic fish with multiple sensors," *International Journal of Advanced Robotic Systems*, vol. 13, no. 62, pp. 1–8, 2016.

[20] J. R. Gottlieb, J. L. Tangorra, and C. J. Esposito, emphet al, "A biologically derived pectoral fin for yaw turn manoeuvres," *Applied Bionics and Biomechanics*, vol. 7, no. 1, pp. 41–55, 2010.

[21] A. J. Ijspeert, A. Crespi, D. Ryczko, and J. M. Cabelguen, "From swimming to walking with a salamander robot driven by a spinal cord model," *Science*, vol. 315, no. 5817, pp. 1416–1420, 2007.

[22] Z. Wu, J. Yu, M. Tan, *et al*, "Kinematic comparison of forward and backward swimming and maneuvering in a self-propelled subcarangiform robotic fish," *Journal of Bionic Engineering*, vol. 11, no. 2, pp. 199–212, 2014.

[23] X. Yang, Z. Wu, and J. Yu, "Design of a camera stabilizer system for robotic fish based on feedback-feedforward control," in Proc. *Chinese Control Conference*, Chengdu, China, Jul. 2016, pp. 6044–6049.

[24] J. Yuan, J. Yu, Z. Wu, *et al*, "Precise planar motion measurement of a swimming multi-joint robotic fish," *Science China Information Sciences*, vol. 59, no. 9, pp. 92208, 2015.